THE ASTROPHYSICAL JOURNAL, 300:258–278, 1986 January 1

METALLICITY DETERMINATIONS FOR GLOBULAR CLUSTERS THROUGH SPECTROPHOTOMETRY OF THEIR INTEGRATED LIGHT

JEAN P. BRODIE
Institute of Astronomy, Cambridge University
AND
DAVID A. HANES
Anglo-Australian Observatory, Epping, Australia
Received 1984 August 29; accepted 1985 June 28

ABSTRACT

Using an appropriately weighted combination of 16 indices of absorption line strength measured in low-dispersion spectra of the integrated light of globular clusters, we determine metallicities [Fe/H] for thirty-six clusters in our own Galaxy. Our results confirm the suggestion that Zinn's (1980) scale suffers a systematic error in the region of intermediate metallicity and support an explanation in which his metallicity-indicative Q_{39} index has been diluted by excess ultraviolet light in clusters with anomalously rich blue horizontal branches. Our methods, which involve the measurement of spectral features arising from many species, produce estimates of metallicity which are insensitive to this problem. We find good agreement with several recent studies, but note a disagreement for the most metal-rich clusters studied by Frogel, Cohen, and Persson (1983). Finally, we apply a similar method with a modified calibration to determine metallicities for the nuclei of six galaxies.

Subject headings: clusters: globular — galaxies: Milky Way — galaxies: nuclei — spectrophotometry — stars: abundances

I. INTRODUCTION

Globular clusters are believed to be among the oldest radiant objects in the universe and may be remnants of the earliest epoch of star formation. As such, they may be useful probes of the dynamical and chemical evolution of galaxies. However, at the distance of most galaxies, individual stars are unresolved in globular clusters, and the determination of the mix of stellar populations and the metal abundance of a cluster must rely upon analysis of its integrated light. In this paper we describe the acquisition of low-resolution spectra of the integrated light of globular clusters in our Galaxy and the subsequent analysis of these data to establish a reliable method of abundance determinations based upon the strengths of certain spectral features. In a companion paper (Hanes and Brodie 1986) we will apply our methods to the interpretation of spectra acquired for several of the globular clusters associated with the giant elliptical galaxy NGC 4486 (M87). Globular cluster populations have now been identified in many galaxies (Harris 1983) and provide rich samples for subsequent spectroscopic analysis (Hesser *et al.* 1984). The Hubble Space Telescope will permit the study of these important objects in many remote galaxies (Bahcall 1984) and shed light upon the earliest stages of galaxy formation and chemical enrichment.

This paper will take the following form. In § II we describe the observational techniques. In § III we describe the data reduction and define the spectroscopic features which we shall employ as metallicity indicators. In § IV we address the question of absolute calibration and derive metallicities for all clusters observed; in § IV*g* we consider the spectra of a few (more metal-rich) galaxies. In § V we compare our results with those of other authors. We confirm the presence of a systematic error in the Zinn (1980) metallicity scale, an error which has been ascribed to the variable contribution of the blue horizontal branch in clusters of similar metallicity, and we test our own results for any sensitivity to such errors. Finally, in § VI we summarize our principal results. We have briefly reported elsewhere (Brodie and Hanes 1981) a preliminary version of our findings; the present paper supersedes those results because of the recent important revisions in the absolute metallicity scale for the globular clusters.

II. OBSERVATIONS

The data analyzed in the present paper were acquired in three observing sessions, summarized in Table 1. Here we describe the important differences between the observing sessions.

a) Lick Observatory

We used the Mark 1 Wampler scanner at the Cassegrain focus of the Lick Observatory 61 cm reflector to acquire spectra at low dispersion of the integrated light of 24 globular clusters and of the nuclei of six bright galaxies. We used a 600 line mm^{-1} grating blazed at 5000 Å in the first order. The projected width of a 7″ slit, convolved with the broad low-

TABLE 1

OBSERVING SESSIONS

OBSERVING FEATURE	SESSION	
	Lick 1978	AAT 1979/1982
Date	May 22/23–Jun 7/8	1979 Mar 25/26–26/27; 1982 Jun 18/19–19/20
Telescope	61 cm Lick	3.9 m AAT
Detector	Mark 1 IDS	IPCS
Resolution	~12 Å	~5 Å

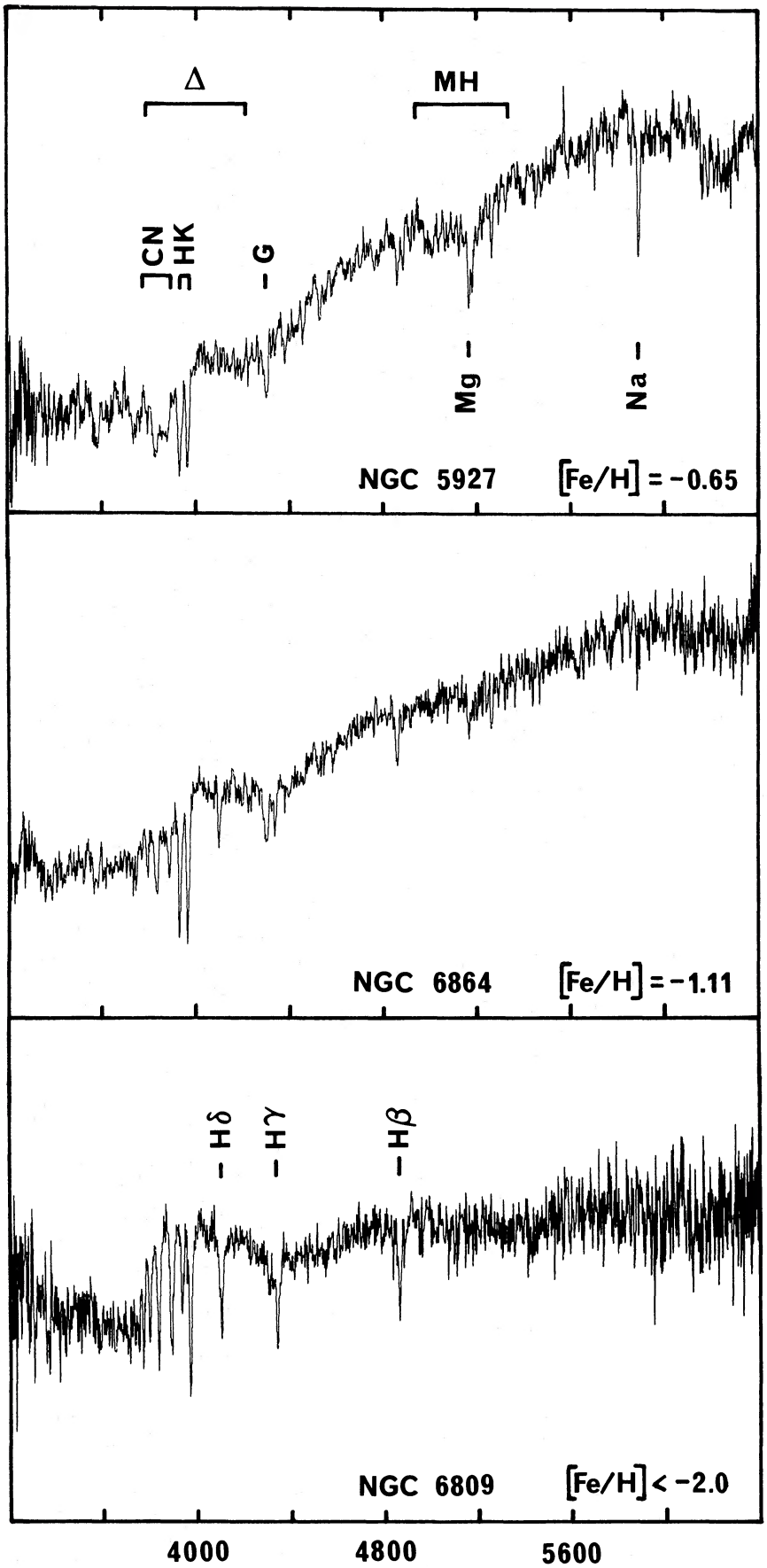

FIG. 1.—Representative spectra for the integrated light of three globular clusters spanning the range of metallicities seen. The ordinate scale is linear, in arbitrary units; the zero point for each spectrum is shown. Several prominent absorption features are marked.

intensity wings of the detector (S. M. Faber 1978, private communication), yielded an effective resolution of ~ 12 Å with ~ 2400 Å coverage in a first-order spectrum. Numerous integrations typically totaling 3600 s on individual clusters were interspersed with frequent observations of emission-line lamps for wavelength calibration and of spectrophotometric standard stars (R. P. Stone 1978, private communication). During the integrations on globular clusters, we occasionally stepped the telescope a few arcseconds perpendicular to the long axis of the spectrograph slit in order to yield a representative mix of the light of the clusters. Each of the two entrance slots, between which we beam-switched the object at frequent intervals, was delimited by dekkers to a length of 80″; they were separated by $\sim 100''$, edge to edge. The data reduction followed conventional practice.

b) *Anglo-Australian Telescope Observations*

We used the image photon counting system (IPCS) at the 25 cm camera of the Royal Greenwich Observatory (RGO) spectrograph (which was attached to the f/8 Cassegrain focus of the 3.9 m Anglo-Australian Telescope [AAT]); with a 250 line mm^{-1} grating, a slit width of 1.″3 projected to ~ 7 Å at the detector. Generally, a smaller slit was used, so that the resolution (~ 5 Å) was effectively set by the detector itself. The telescope was nodded perpendicular to the long slit and typically through 30″ sweeps over the face of each cluster to yield a spectrum of the integrated light. Occasionally the night-sky contribution was determined via a separate integration, but more generally we carried out simultaneous cluster and sky observations at either end of the long ($>3'$) slit. We observed 17 clusters in this fashion, and calibrated their continuum flux distributions with reference to the standard stars (Oke 1974) customarily used at the AAT.

III. DEFINITION AND MEASUREMENT OF FEATURE STRENGTHS

In Figure 1 we present representative spectra for three globular clusters spanning a wide range of heavy-element abundance, as shown. Simple inspection reveals the presence of a number of prominent absorption features whose strength is a function of metallicity. Following Brodie (1980), we have identified a set of 16 such features, which we measure as follows: denote by F_λ the flux per channel at a wavelength λ. Define $F(\lambda_1, \lambda_2)$ as the total flux and $\bar{F}(\lambda_1, \lambda_2)$ as the average flux per unit wavelength in the interval (λ_1, λ_2), i.e.,

$$\bar{F}(\lambda_1, \lambda_2) = \frac{1}{\lambda_2 - \lambda_1} \int_{\lambda_1}^{\lambda_2} F_\lambda \, d\lambda = \frac{F(\lambda_1, \lambda_2)}{(\lambda_2 - \lambda_1)} . \quad (1)$$

Then, following Norris (1980), we introduce a generalized index I:

$$I\,[= I(\lambda_1, \lambda_2, \lambda_3, \lambda_4)] = 1.0 - \frac{2\bar{F}(\lambda_2, \lambda_3)}{\bar{F}(\lambda_1, \lambda_2) + \bar{F}(\lambda_3, \lambda_4)} . \quad (2)$$

So defined, I is a measure of the flux per unit wavelength interval within the window relative to its mean value in two sidebands. It is normalized so that $I = 0$ corresponds to a smoothly sloping featureless continuum, while $I = 1.0$ corresponds to a black window in such a continuum.

We define one additional index, Δ, as follows:

$$\Delta = 2.5 \log \left[\frac{F(4000, 4200)}{F(3800, 4000)} \right] . \quad (3)$$

It is a measure of the continuum step near 4000 Å arising from Fraunhofer line blocking shortward of that wavelength. Van den Bergh and Henry (1962) first introduced a closely similar index Δ, measured in a rather subjective fashion, and showed that it correlated strongly with the mean metallicity of globular clusters. Zinn's (1980) Q_{39} metallicity indicator has a similar operational definition. In Table 2 we present the definition of all of our indices and identify the species which give rise to the observed variations in feature strength.

Necessary preliminaries to the measurement of feature strengths include the correction of the observed spectrum for the effects of interstellar reddening and a correction for systemic velocity to bring the features to the rest-wavelength frame. For the reddening corrections, values of E_{B-V} were taken from the tabulation of Harris and Racine (1979). (Reddenings for the few galaxies observed were derived from the modified cosecant law of Sandage 1973.) The Lick data were corrected using a polynomial representing a digitized version of van de Hulst's curve 15 (Johnson 1968); for the AAT data we used an equivalent procedure which is embodied in the Anglo-Australian Observatory's SDRSYS spectroscopic data reduction system. For correction to the rest frame, we took velocities from Madore's (1980) compilation for the globular clusters and from the *Second Reference Catalogue of Bright Galaxies* (de Vaucouleurs, de Vaucouleurs, and Corwin 1976) for galaxies. For three clusters (NGC 5634, NGC 5946, and NGC 6352) no velocities were known, so no correction was applied.

Because of the generally small wavelength range over which the indices were measured, the effect of errors in the tabulations of interstellar reddening is likely to be negligible, even for Δ. Harris and Racine (1979) quote a typical error of ± 0.04 in E_{B-V}, which translates to a formal error of ± 0.007 in Δ; the photon-statistical error is generally larger than this. Indeed, uncertainties in the stability of the atmospheric extinction may be a slightly larger source of uncertainty in determinations of Δ. Similarly, the lack of systematic velocities for a few clusters is unlikely to have a significant effect on the measured indices because the shifts are small.

In Table 3 are to be found all measured indices for the globular clusters studied at Lick and the AAT. In Table 3A we present the results from Lick, with multiple entries for any clusters observed more than once. The last column lists

TABLE 2

DEFINITION OF INDICES

Index	λ_1	λ_2	λ_3	λ_4
Δ (UV blanketing)	3800	4000	4000	4200
H_{10} (Balmer line)	3785	3795	3810	3825
H_9 (Balmer line)	3810	3825	3850	3865
Hζ (Balmer line)	3865	3885	3910	3925
CN (UV cyanogen)	3785	3810	3910	3925
HK (Ca II H and K lines)	3910	3925	3995	4015
Hδ (Balmer line)	4075	4090	4125	4140
Ca (Ca I line)	4200	4215	4245	4260
G (CH G band)	4275	4285	4315	4325
Hγ (Balmer line)	4315	4325	4360	4375
Hβ (Balmer line)	4800	4830	4890	4920
Mg (Mg *b* triplet)	5125	5150	5195	5220
MH (Mg *b* + MgH)	4740	4940	5350	5550
FC (Fe I + Ca I)	5225	5250	5280	5305
Na (Na D lines)	5385	5865	5920	5950
FTC (Fe I + TiO + Ca I)	5950	6100	6330	6480
Hα (Balmer line)	6480	6515	6575	6610

TABLE 3A

INDICES FOR GLOBULAR CLUSTERS OBSERVED AT LICK

NGC	M	Δ	H_{10}	H_9	$H\zeta$	CN	HK	$H\delta$	Ca	G	$H\gamma$	$H\beta$	Mg	MH	FC	Na	$H\alpha$	FTC	wt
5024	53	0.149	0.090	0.079	0.089	-0.019	0.124	0.059	-0.010	0.043	0.066	0.054	0.006	0.014	0.013	0.013	0.015	0.019	2.9
		0.226	0.034	0.201	0.141	0.017	0.165	0.003	0.018	0.069	0.063	0.047	-0.015	0.011	0.022	-	-	-	0.6
5272	3	0.222	0.081	0.127	0.072	0.011	0.151	0.069	0.000	0.060	0.060	0.045	0.012	0.023	0.023	0.007	0.027	0.021	8.0
5634		0.229	0.174	0.113	0.070	-0.049	0.150	0.087	0.014	0.035	0.062	0.038	0.015	0.020	0.004	-	-	-	1.4
		0.230	0.066	0.293	0.119	0.125	0.205	0.122	-0.003	0.000	0.099	0.050	0.007	0.017	0.005	-	-	-	0.8
5904	5	0.290	0.061	0.132	0.093	0.051	0.200	0.067	0.015	0.061	0.044	0.051	0.025	0.028	0.025	0.012	0.006	0.022	9.2
		0.245	0.086	0.080	0.144	0.065	0.191	0.092	-0.008	0.044	0.076	0.060	0.024	0.011	0.022	-	-	-	0.8
6093	80	0.203	0.058	0.077	0.143	0.016	0.162	0.069	0.009	0.025	0.042	0.040	0.014	0.010	0.020	-	-	-	6.9
6171	107	0.435	-0.014	-0.042	0.068	0.110	0.245	-0.002	0.024	0.049	0.040	0.033	0.038	0.041	0.024	0.028	0.021	0.055	0.8
		0.403	0.088	-0.199	0.400	0.295	0.319	0.172	-0.059	-0.015	0.015	0.066	0.015	0.019	0.025	-	-	-	0.2
6205	13	0.248	0.052	0.131	0.117	0.054	0.185	0.069	0.006	0.057	0.061	0.047	0.010	0.021	0.017	0.019	0.025	0.025	4.7
6218	12	0.319	-0.047	0.023	0.107	0.036	0.159	0.053	0.007	0.058	0.038	0.042	0.029	0.030	0.011	0.020	0.004	0.031	1.1
		0.227	0.048	0.159	0.125	0.126	0.140	0.066	0.024	0.020	0.029	0.051	0.027	0.020	0.045	-	-	-	0.7
6229		0.296	0.104	0.128	0.072	0.037	0.201	0.044	0.012	0.069	0.070	0.039	0.027	0.023	0.024	-	-	-	2.5
6254	10	0.223	0.073	0.067	0.128	0.064	0.155	0.095	0.023	0.036	0.079	0.032	0.019	0.019	0.032	0.029	0.017	0.018	1.8
6273	19	0.253	-0.014	0.087	0.088	0.000	0.163	0.041	0.011	0.024	0.056	0.044	0.011	0.023	0.017	-	-	-	1.6
6341	92	0.173	0.043	0.070	0.085	0.002	0.129	0.068	0.012	0.012	0.053	0.043	0.015	0.008	0.011	0.005	0.018	0.019	4.9
6356		0.520	-0.175	0.012	0.050	0.158	0.249	-0.064	0.013	0.058	-0.030	0.032	0.049	0.053	0.032	0.057	0.005	0.054	2.8
		0.547	0.030	0.178	0.034	0.236	0.307	0.009	-0.003	0.084	0.016	0.032	0.052	0.055	0.041	-	-	-	2.0
6402	14	0.310	0.169	0.188	0.062	0.013	0.151	0.050	-0.005	0.015	0.006	0.059	0.015	0.030	0.025	-	-	-	0.8
		0.218	0.002	-0.139	0.088	0.028	0.321	0.051	-0.001	0.037	0.003	0.039	0.014	0.025	0.032	0.047	0.016	0.039	0.1
6626	28	0.356	0.119	0.094	0.117	0.057	0.201	0.036	0.002	0.036	0.009	0.024	0.032	0.026	0.033	0.026	0.000	0.039	2.9
6712		0.411	-0.093	0.038	0.079	0.108	0.206	0.024	0.001	0.044	0.017	0.044	0.033	0.034	0.030	-	-	-	0.7
		0.320	0.120	0.040	0.009	-0.059	0.314	0.010	0.092	0.052	0.099	0.021	0.029	0.038	0.030	-	-	-	0.6
6779	56	0.226	-0.039	0.051	0.082	0.041	0.186	0.076	-0.007	0.016	0.077	0.044	0.011	0.013	0.002	0.025	0.017	0.024	1.0
6838	71	0.546	0.067	0.165	-0.043	0.114	0.249	0.016	-0.009	0.097	-0.008	0.045	0.033	0.063	0.033	-	-	-	0.8
		0.391	0.024	0.301	0.134	0.057	0.140	0.106	0.057	0.083	0.090	0.036	0.052	0.048	0.023	-	-	-	0.3
6864	75	0.372	0.137	0.071	0.070	0.047	0.221	-0.015	0.017	0.063	0.057	0.033	0.017	0.023	0.031	-	-	-	2.9
6934		0.274	0.110	0.101	0.130	0.028	0.184	0.075	-0.007	0.078	0.063	0.042	0.032	0.017	0.024	-	-	-	2.2
6981	72	0.236	0.265	0.021	0.160	0.238	0.150	0.100	0.055	0.018	0.060	0.040	0.014	0.020	0.040	-	-	-	0.2
7006		0.248	0.270	0.152	0.121	-0.023	0.197	-0.001	-0.003	0.014	0.029	0.060	0.011	0.024	0.015	-	-	-	0.6
7078	15	0.175	0.073	0.044	0.105	-0.013	0.114	0.076	-0.002	0.006	0.050	0.043	0.015	0.005	0.011	0.021	0.027	0.017	6.5
7089	2	0.243	0.074	0.038	0.096	0.008	0.150	0.039	0.023	0.014	0.064	0.049	0.020	0.013	0.020	-	-	-	4.2

TABLE 3B

INDICES FOR GLOBULAR CLUSTERS OBSERVED AT AAT

NGC	M	Δ	H_{10}	H_9	Hζ	CN	HK	Hδ	Ca	G	Hγ	Hβ	Mg	MH	FC	Na	Hα	FTC
1851		0.348	0.066	0.180	0.071	0.079	0.254	0.050	0.025	0.106	0.085	0.036	0.027	0.033	0.049	0.028	0.032	0.018
		(6)	(20)	(16)	(14)	(11)	(10)	(11)	(11)	(12)	(11)	(7)	(9)	(3)	(11)	(11)	(15)	(6)
1904	79	0.213	0.130	0.194	0.114	0.041	0.178	0.135	-0.020	0.088	0.089	0.074	0.006	-0.006	0.013	0.021	0.023	0.006
		(4)	(12)	(10)	(9)	(7)	(7)	(8)	(8)	(10)	(9)	(7)	(9)	(3)	(11)	(12)	(17)	(7)
2298		0.177	0.079	0.178	0.121	0.049	0.182	0.102	-0.039	0.004	0.080	0.065	0.055	0.010	0.061	0.032	0.072	0.052
		(11)	(39)	(32)	(28)	(21)	(21)	(23)	(22)	(26)	(24)	(16)	(20)	(7)	(23)	(24)	(32)	(13)
5927		0.577	-0.083	0.173	-0.126	0.214	0.282	-0.010	-0.037	0.196	0.011	0.068	0.117	0.066	0.057	0.087	0.032	0.044
		(10)	(36)	(36)	(25)	(20)	(17)	(15)	(15)	(16)	(13)	(8)	(10)	(3)	(11)	(11)	(14)	(6)
5946		0.288	0.134	0.196	0.091	0.037	0.240	0.121	0.013	0.072	0.124	0.070	0.022	0.019	0.051	0.054	0.016	0.016
		(7)	(28)	(22)	(18)	(14)	(13)	(13)	(12)	(14)	(13)	(8)	(9)	(3)	(10)	(11)	(15)	(6)
5986		0.253	0.162	0.174	0.109	0.048	0.213	0.097	0.014	0.098	0.088	0.066	0.031	0.015	0.048	0.037	0.013	0.016
		(5)	(18)	(14)	(12)	(9)	(9)	(10)	(9)	(11)	(9)	(6)	(8)	(3)	(10)	(11)	(16)	(6)
6352		0.526	-0.143	0.155	-0.042	0.124	0.244	0.002	-0.024	0.180	0.017	0.057	0.070	0.022	0.080	0.079	-0.027	-0.007
		(13)	(51)	(45)	(35)	(27)	(24)	(21)	(21)	(25)	(22)	(13)	(17)	(6)	(19)	(24)	(34)	(12)
6356		0.566	0.001	0.192	-0.080	0.194	0.317	0.021	0.018	0.193	0.032	0.046	0.065	0.053	0.077	0.069	0.022	0.019
		(6)	(22)	(21)	(16)	(12)	(11)	(10)	(10)	(11)	(10)	(6)	(8)	(3)	(9)	(9)	(12)	(5)
6362		0.421	0.007	0.234	0.063	0.108	0.250	0.065	0.064	0.182	0.016	0.065	0.062	0.050	0.100	0.096	-0.049	0.051
		(17)	(58)	(59)	(48)	(33)	(30)	(29)	(28)	(30)	(26)	(16)	(20)	(7)	(22)	(29)	(31)	(14)
6541		0.221	0.097	0.164	0.077	0.045	0.200	0.084	0.016	0.069	0.072	0.069	0.024	0.011	0.026	0.021	0.032	-0.010
		(4)	(12)	(10)	(9)	(6)	(6)	(7)	(7)	(8)	(8)	(6)	(7)	(3)	(9)	(11)	(16)	(6)
6712		0.398	0.046	0.162	0.003	0.127	0.243	-0.002	0.003	0.166	0.059	0.054	0.073	0.035	0.029	0.049	0.068	0.020
		(8)	(32)	(27)	(22)	(17)	(16)	(16)	(15)	(17)	(15)	(9)	(11)	(4)	(12)	(13)	(18)	(7)
6723		0.339	0.002	0.173	0.035	0.069	0.222	0.037	0.027	0.140	0.037	0.056	0.038	0.018	0.068	0.041	0.044	-0.012
		(7)	(23)	(20)	(17)	(13)	(13)	(14)	(14)	(16)	(15)	(12)	(15)	(6)	(20)	(24)	(39)	(15)
6752		0.231	0.096	0.175	0.109	0.074	0.222	0.098	0.012	0.095	0.090	0.077	0.051	0.013	0.039	0.011	0.048	0.003
		(4)	(14)	(11)	(10)	(8)	(8)	(8)	(8)	(10)	(9)	(7)	(10)	(3)	(11)	(14)	(26)	(8)
6809	55	0.131	0.115	0.209	0.168	0.029	0.177	0.128	0.006	0.002	0.116	0.109	0.026	0.004	0.000	-0.053	-0.035	0.021
		(8)	(27)	(20)	(19)	(14)	(14)	(17)	(16)	(19)	(18)	(15)	(19)	(7)	(23)	(32)	(51)	(18)
6838	71	0.540	-0.070	0.106	0.005	0.113	0.281	0.046	-0.002	0.200	0.010	0.072	0.111	0.058	0.068	0.053	-0.022	0.017
		(12)	(47)	(42)	(33)	(25)	(23)	(20)	(19)	(22)	(18)	(11)	(14)	(5)	(15)	(18)	(25)	(10)
6864	75	0.332	0.056	0.189	0.094	0.072	0.252	0.074	0.031	0.144	0.066	0.041	0.038	0.024	0.044	0.015	0.026	0.005
		(5)	(18)	(15)	(13)	(10)	(10)	(10)	(10)	(12)	(11)	(8)	(10)	(3)	(12)	(13)	(20)	(8)
6981	72	0.273	0.033	0.156	0.069	0.038	0.212	0.104	0.044	0.090	0.064	0.067	0.029	0.023	0.059	0.036	0.018	0.009
		(7)	(24)	(19)	(17)	(13)	(13)	(14)	(14)	(16)	(14)	(10)	(13)	(4)	(15)	(20)	(30)	(11)

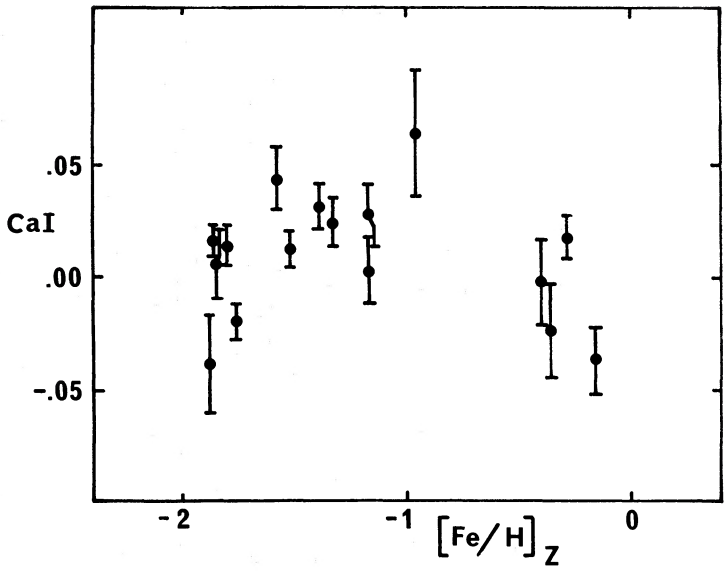

FIG. 2.—Behavior of the Ca I index as a function of cluster metallicity as given by Zinn (1980). Error bars are those implied by photon-statistical considerations only. Data are from the AAT observing sessions.

weights assigned by Brodie (1980) to individual spectra according to objective signal-to-noise estimates. In Table 3B we present the results from the AAT sessions. For those measurements no weights are tabulated; rather, the formal photon-statistical error is given in parentheses below each entry.

Before considering the calibration of the data given in Table 3, we show in Figure 2 the particular behavior of our Ca index as a function of the metallicity of globular clusters (taken from Zinn 1980). It is not a monotonic function of abundance, presumably because of contaminating absorption features in the sidebands as they were originally defined (Brodie 1980), so we do not consider this index further.

IV. CALIBRATION

a) Fundamental Calibrators

The globular cluster metallicity scale has lately been controversial (Pilachowski 1984; Frogel, Cohen, and Persson 1983; Peterson 1983; Bessell 1983). The implications of proposed revisions, especially in the high-metallicity regime, are far-reaching (Freeman and Norris 1981). A recent summary of the state of the subject is provided by Pilachowski (1984). Here we adopt the metallicities of those clusters observed by us which have entries in Pilachowski's Table 1 under the heading "Calibration." We note that she assigns a metallicity of [Fe/H] = −0.8 to the important metal-rich cluster NGC 6838 (M71). This value is significantly lower than the long-accepted value [Fe/H] = −0.4 but represents a smaller downward revision than that originally suggested by Cohen (1980), who derived [Fe/H] = −1.3; however, Cohen (1983) has herself more recently redetermined the metallicity of M71 to lie near [Fe/H] = −0.7. The question is not yet completely resolved, and, as in any study of this nature, our scale will be sensitive to future revisions. With this proviso, we summarize in Table 4 the clusters which make up our set of fundamental calibrators—those for which the metallicity is precisely known on the basis of the spectroscopic study of individual member stars.

b) Comparison of the Sets of Observations

Unfortunately only a few clusters were observed both at the Lick Observatory and at the AAT. Most of those were moderately metal-rich, and it is not possible directly to intercompare measurements of all indices at the two sites for enough clusters over a wide enough range in metallicity to establish their complete consistency.

We may, however, compare the measurements through the

TABLE 4

CALIBRATING CLUSTERS

NGC	Messier	[Fe/H]	NGC	Messier	[Fe/H]
1851.....	...	−1.07 ± 0.2	6254.....	10	−1.32 ± 0.15
1904.....	79	−1.43 ± 0.2	6341.....	92	−2.12 ± 0.15
2298.....	...	−1.5 ± 0.3	6362.....	...	−0.98 ± 0.2
5024.....	53	−1.88 ± 0.2	6402.....	14	−1.11 ± 0.25
5272.....	3	−1.57 ± 0.1	6723.....	...	−1.10 ± 0.3
5634.....	...	−1.61 ± 0.25	6752.....	...	−1.32 ± 0.2
5904.....	5	−1.15 ± 0.15	6838.....	71	−0.8 ± 0.1
6171.....	107	−0.94 ± 0.2	6981.....	72	−1.27 ± 0.25
6205.....	13	−1.44 ± 0.15	7078.....	15	−1.90 ± 0.2
6229.....	...	−1.3 ± 0.3	7089.....	2	−1.43 ± 0.15

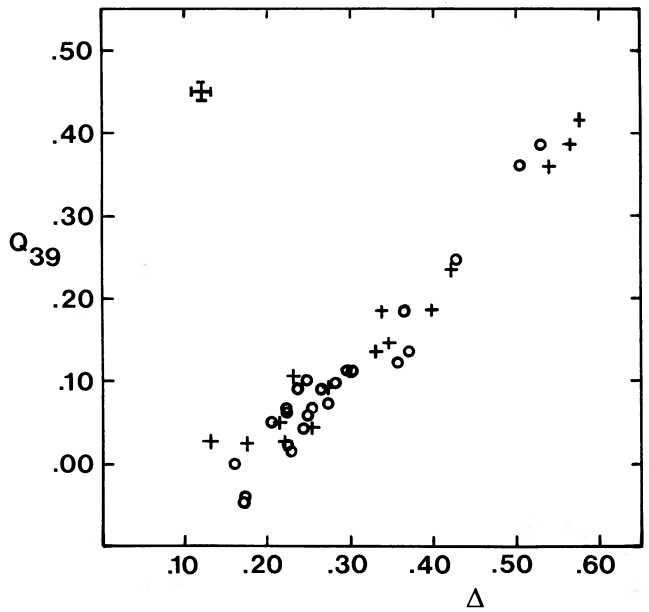

FIG. 3.—Relationship between our Δ index and the Q_{39} index measured by Zinn (1980) for clusters in common. Open circles represent data from Lick Observatory; plus signs represent data from the AAT. A typical error bar is shown at the upper left.

use of an independent parameter which allows a rank ordering of clusters according to metallicity. Such a comparison is shown in Figure 3, in which we plot Zinn's (1980) metallicity-dependent Q_{39} index against the Δ index measured by us. The good mingling of our separate data sets reassures us of the consistency of our observations at the two sites. The MH index reveals good agreement as well, as is shown in Figure 4, although there is just a hint of a slight separation in the metal-poor regime. Apparently, however, the large-scale features Δ and MH are consistently measured regardless of observing site or instrument, despite the fact that different flux standard stars were used at the two sites.

The agreement does not persist to indices defined over smaller wavelength intervals. In Figure 5 we show, for example, that the HK feature strength as measured at Lick Observatory is systematically weaker than as measured at the AAT. We plausibly ascribe this effect to the washing out of narrow features in the lower resolution Lick spectra.

c) Calibration Techniques

The usual procedure would be to consider each index in turn, plotting measured values against adopted metallicity for the calibrating clusters and thereby deriving the dependence of feature strength upon metallicity. For the Lick data, this procedure would suffice; but for the AAT data, we observed too few of the clusters drawn from Pilachowski's Table 1 to provide formally well-defined calibrations. Nor is it possible simply to combine all the data (except for the Δ and MH indices) because of the systematic differences noted in § IV*b* for the narrower features.

We therefore adopt the following straightforward procedure. For each data set we plot each index in turn against Δ and, through fitted relationships, reduce all indices to an equivalent value of Δ. A suitably weighted average of these estimates represents our final discriminator of cluster metallicity, and has the extra advantage that it is defined in terms of many line-forming species. The transformation to absolute metallicities follows immediately from the adopted fundamental calibrators.

We now consider the treatment of each data set independently.

d) Lick Data

Each index in turn is plotted against Δ in Figure 6*a*–6*o*. Lacking photon-counting spectrophotometry, we cannot assign an absolute error to each measured index. However, we adopt the weights given in Table 3A and symbolize the plotted points accordingly, so that the reader may judge the quality of the correlations. (For clusters measured more than once, a weighted mean of separate determinations is plotted.) Within

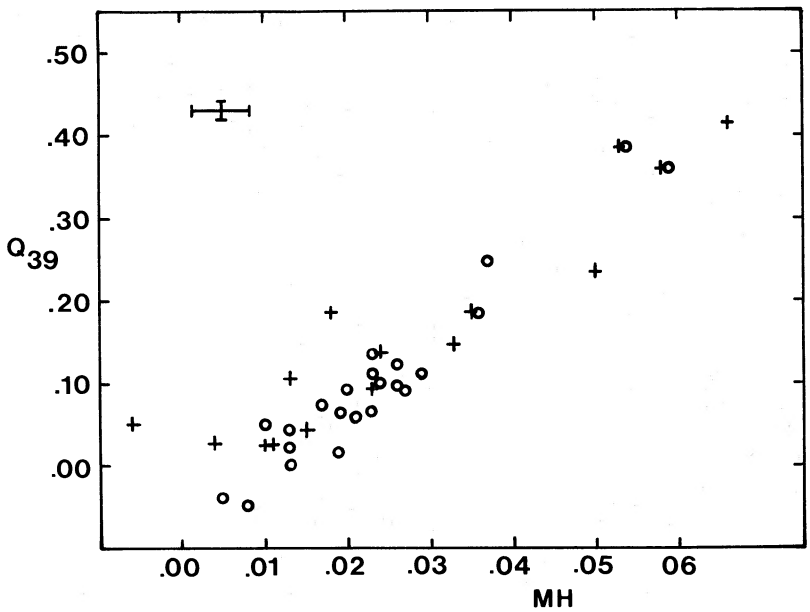

FIG. 4.—Relationship between our MH index and the Q_{39} index measured by Zinn (1980) for clusters in common. Symbols have the same meaning as in Fig. 3.

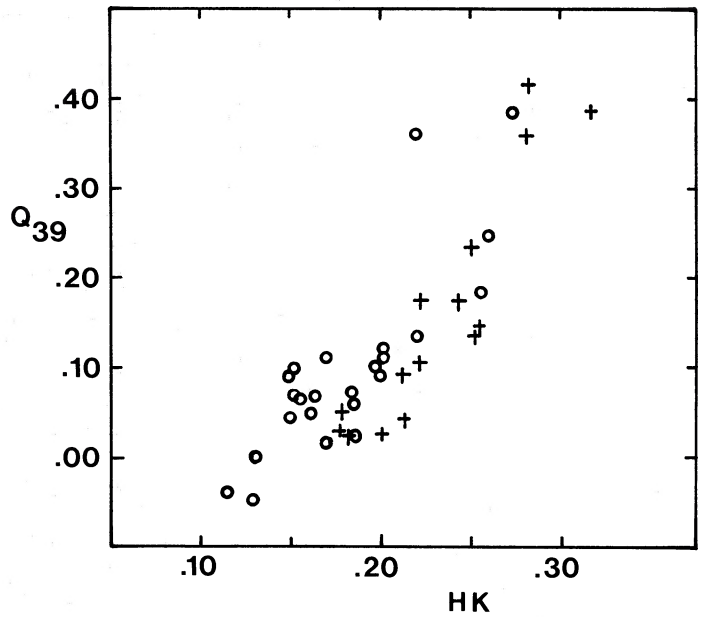

FIG. 5.—Relationship between our HK index and the Q_{39} index measured by Zinn (1980) for clusters in common. Symbols have the same meaning as in Fig. 3.

each subpanel of the figure, the weighted linear correlation coefficient and a weighted linear least-squares relationship are given. For MH only, the regression was made in two senses and an average was taken; for all other relationships, the Δ index was treated as error-free.

Inspection of the panels reveals that most of the non–hydrogen line indices are strongly correlated with Δ and are by inference robust indicators of metallicity. The hydrogen line strengths generally display anticorrelations, in accordance with our expectations that more metal-poor clusters (with enhanced blue horizontal branches) will have stronger Balmer absorption lines.

For each cluster, each measured index I_i now yields an indirect estimate of Δ, denoted Δ_i, and the estimates may be averaged. In the taking of averages, the points must be carefully weighted: when a particular correlation is weak, and the fitted relationship near zero slope, an individual estimate of Δ_i may be grossly in error. Therefore, for each cluster we derive a mean estimate $\bar{\Delta}$ by weighting each separate estimate according to $w_i \propto \tan^2 (r_i \pi/2)$, where r_i is the correlation coefficient between the ith index and Δ. This weighting has the desired property of going to $w = \infty$ as r approaches unity and to $w = 0$ as r approaches zero. It is further empirically justified by tests upon the AAT data, where the absolute error bars, and so precise relative weights, are known. We note by way of example that this weighting means that estimates based upon a correlation with $r = 0.5$ enter with weight 1/40 when estimates from a correlation with $r = 0.9$ are given unit weight.

The exception to our formal weighting is in our treatment of the Δ index itself. It has the doubly unfavorable property of being an asymmetric feature defined over a rather long baseline in wavelength. It is therefore more sensitive to errors in the corrections for reddening and atmospheric extinction than are the other indices, yet it is easily measurable to high precision. Rather than include it with the high weight its formal precision would suggest in the AAT data, or assigning some correspondingly high weight in the Lick analysis, we conservatively assign it a weight equal to that for the mean value derived from all other indices. We will return to this point in § V.

In Table 5 we present the final estimates of $\bar{\Delta}$ derived in this fashion. For each tabulated value, the quoted uncertainty is the standard error of the weighted mean as determined from the

TABLE 5

FINAL ESTIMATES OF $\bar{\Delta}$

A. $\bar{\Delta}$ FROM LICK OBSERVATORY DATA

NGC	$\bar{\Delta}$	NGC	$\bar{\Delta}$
5024	0.174 ± 0.012	6712[a]	0.376 ± 0.006
5272	0.221 ± 0.001	6779	0.231 ± 0.005
5634	0.220 ± 0.009	6838[a]	0.474 ± 0.030
5904	0.263 ± 0.003	6864[a]	0.347 ± 0.026
6093	0.206 ± 0.003	6934	0.270 ± 0.004
6171	0.453 ± 0.025	6981[a]	0.265 ± 0.029
6205	0.251 ± 0.003	7006	0.253 ± 0.005
6218	0.291 ± 0.007	7078	0.171 ± 0.004
6229	0.297 ± 0.001	7089	0.230 ± 0.013
6254	0.220 ± 0.003		
6273	0.245 ± 0.008		
6341	0.179 ± 0.006		
6356[a]	0.532 ± 0.002		
6402	0.319 ± 0.019		
6626	0.358 ± 0.003		

B. $\bar{\Delta}$ FROM AAT DATA

NGC	$\bar{\Delta}$	NGC	$\bar{\Delta}$
1851	0.345 ± 0.004	6712[a]	0.411 ± 0.013
1904	0.194 ± 0.019	6723	0.346 ± 0.007
2298	0.197 ± 0.020	6752	0.244 ± 0.013
5927	0.597 ± 0.020	6809	0.130 ± 0.002
5946	0.271 ± 0.018	6838[a]	0.531 ± 0.009
5986	0.248 ± 0.005	6864[a]	0.327 ± 0.006
6352	0.487 ± 0.039	6981[a]	0.277 ± 0.004
6356[a]	0.554 ± 0.012		
6362	0.446 ± 0.025		
6541	0.229 ± 0.008		

[a] Clusters observed at both sites.

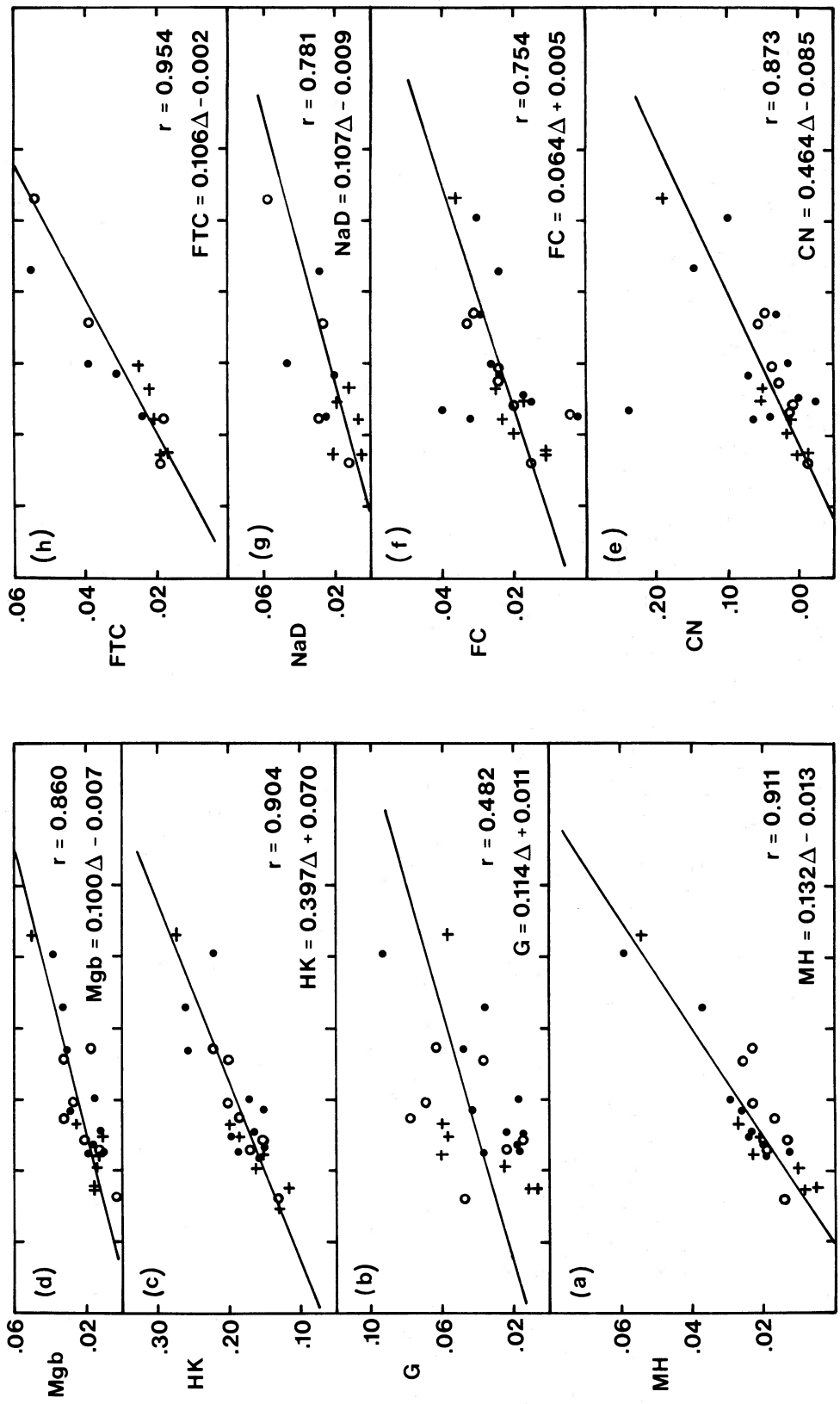

FIG. 6.—(*a–o*) Dependence of each index upon Δ for all clusters observed at Lick. Symbols represent observations of different statistical weights (given in Table 3A): plus signs represent the highest weight data, filled circles the lowest. In each panel is given the weighted linear correlation coefficient and regression line. For all but the G index, the dominant error was assumed to be in the variable plotted on the ordinate; for G, regressions were taken in both senses and averaged.

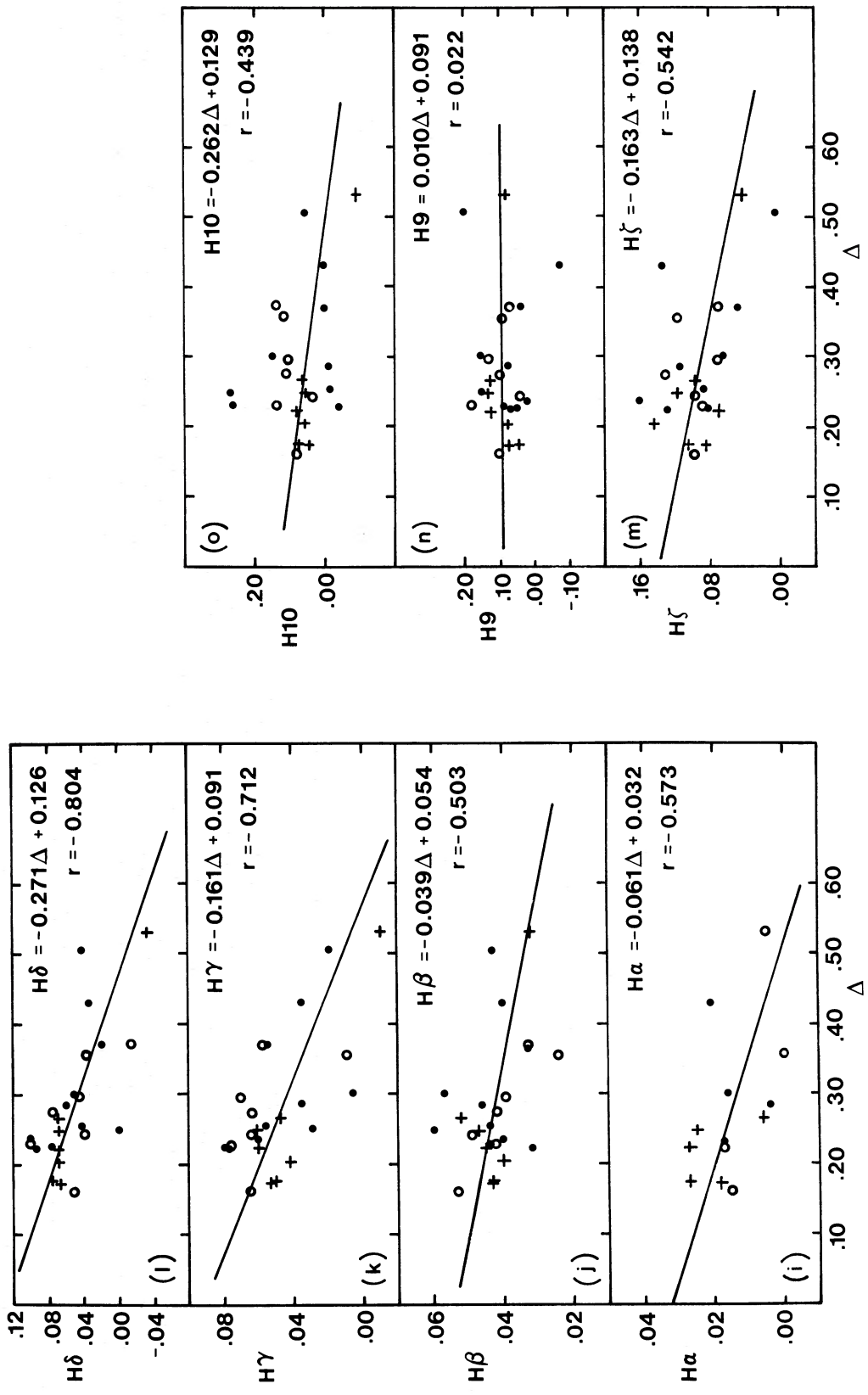

FIG. 6.—*Continued*

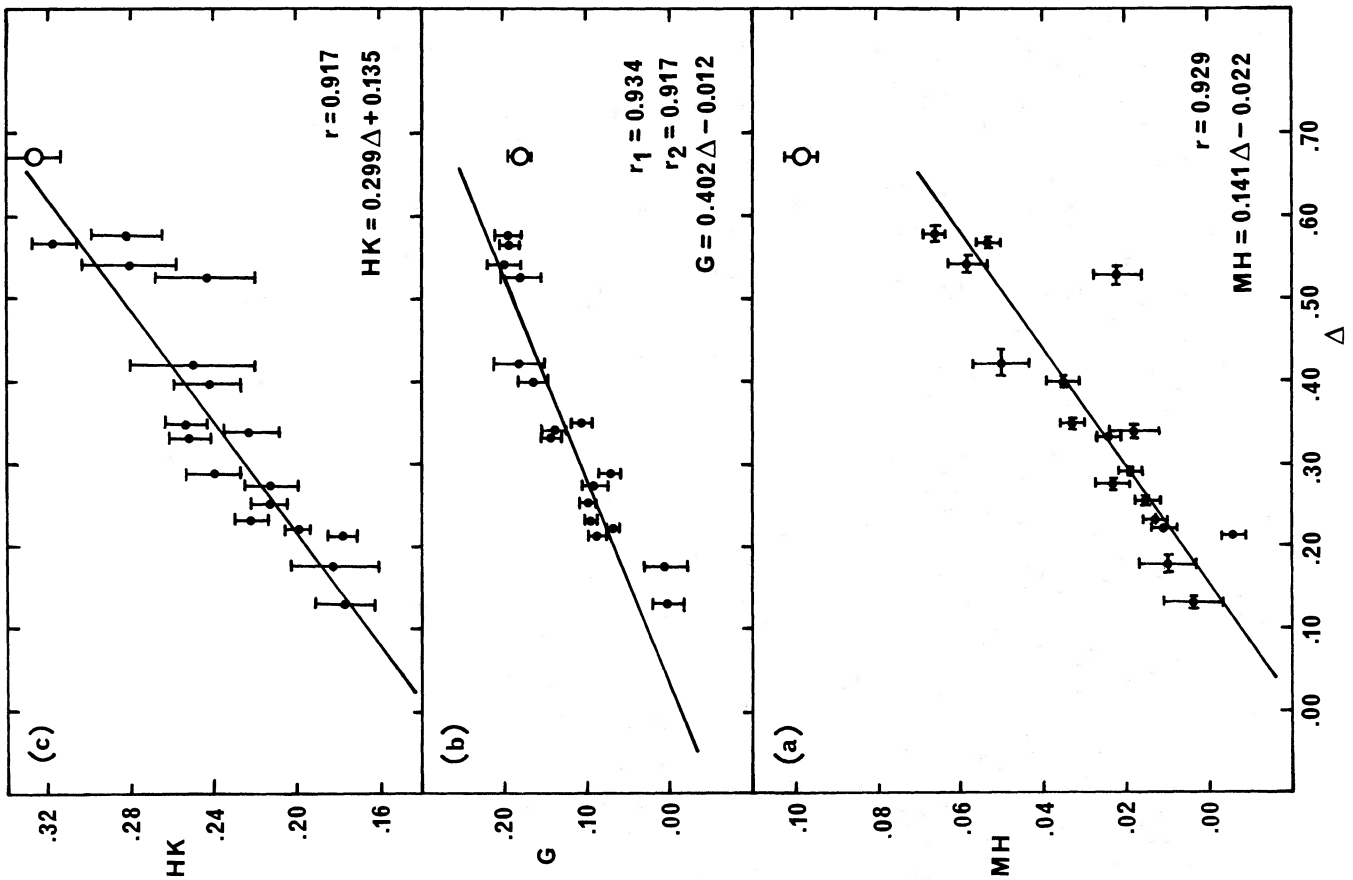

FIG. 7.—(*a–o*) Dependence of each index upon Δ for all clusters observed at AAT. Error bars are those arising from photon statistics alone. The weighted correlation coefficient and weighted linear regression are given in each panel, assuming all the error to be in the variable plotted along the ordinate. When two correlation coefficients are given, they represent the alternative assumptions about the dominant error; in such cases the equation quoted is a mean of the separate determinations. The open symbol, which represents the nucleus of NGC 4486 (M87), was not included in the regression.

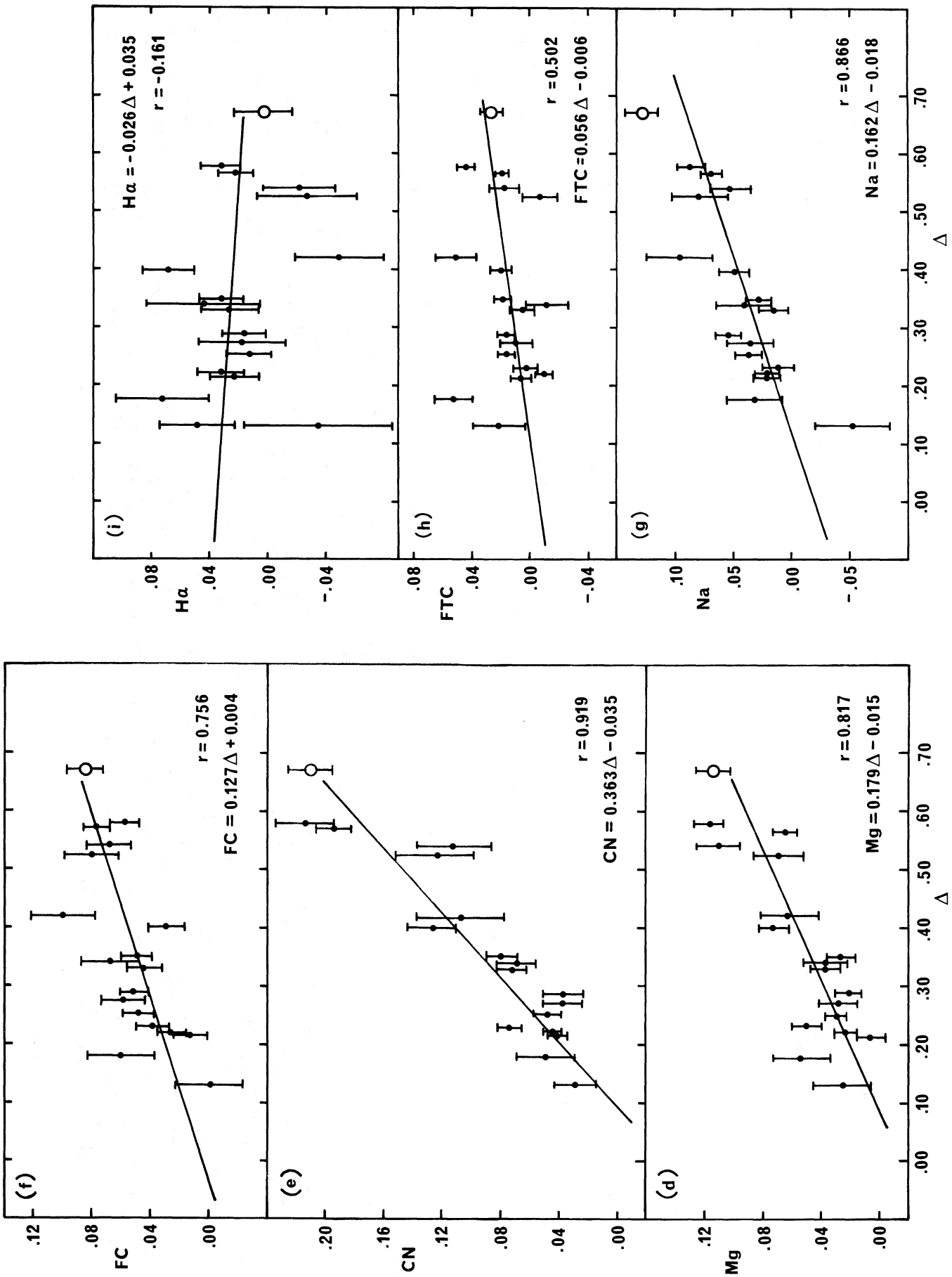

FIG. 7.—*Continued*

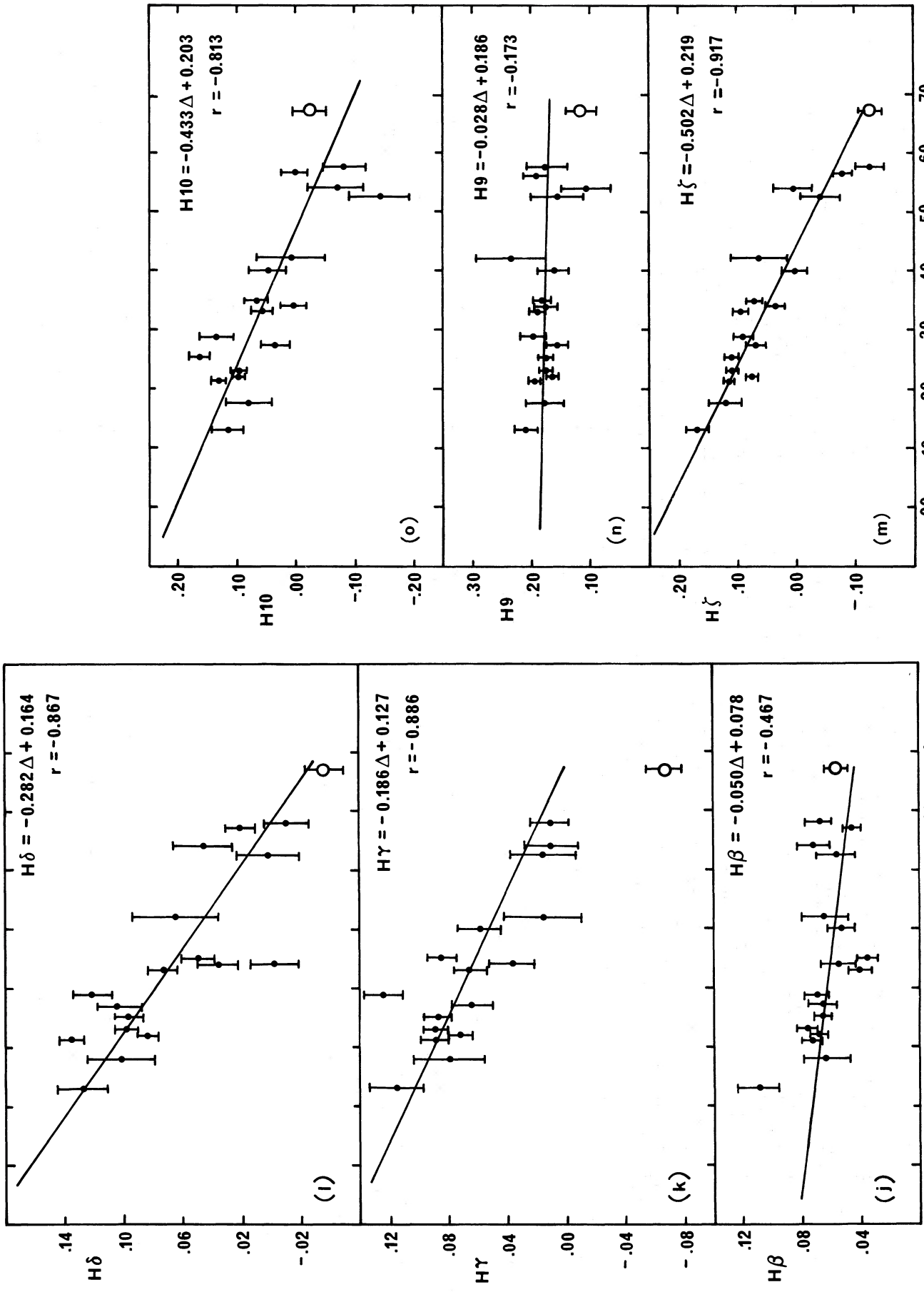

FIG. 7.—*Continued*

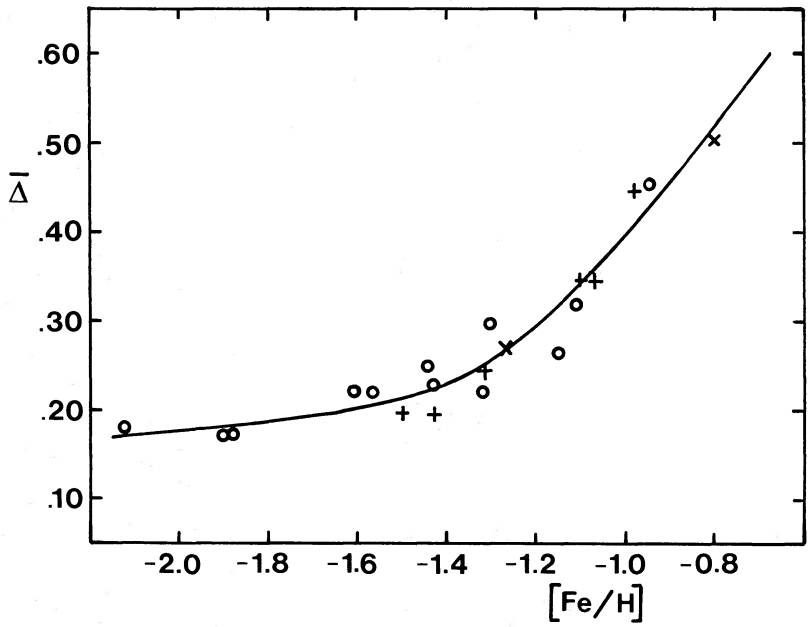

FIG. 8.—Dependence of the mean index $\bar{\Delta}$, derived as described in the text, upon metallicity for the 20 fundamental calibrating clusters given in Table 4. Open circles represent clusters observed only at Lick; plus signs represent clusters observed only at AAT; and crosses represent clusters observed at both sites. The smooth curve is our freehand fit to the data.

formal agreement of the various estimates. We emphasize here that the table quotes these internal errors only; the true systematic uncertainties must be somewhat larger.

e) AAT Data

In the panels of Figures 7*a*–7*o* we present plots for each measured index as a function of Δ. The correlation coefficients and fitted relationships were derived by weighting each point according to the inverse square of its photon-statistical error (excluding the open circle in each panel, which represents the nucleus of M87). For the G index alone the regression was carried out in two senses and the mean was adopted.

As for the Lick data, we find that the indices are strongly correlated (or anticorrelated, for the Balmer lines) with Δ; generally the relationships are of similar robustness within the AAT and the Lick data. The open circle representing the nucleus of M87 demonstrates that this galaxy generally lies on the metal-rich extrapolation of the relationships, a point to which we return in § IV*g*. As in the Lick analysis, we now use the measured strength I of each index to predict an equivalent Δ_i, with formal uncertainties. We then calculate a weighted mean $\bar{\Delta}$ for each cluster, recording it in Table 5*b*.

f) Cluster Metallicities

Inspection of Table 5 reveals that estimates of $\bar{\Delta}$ from clusters measured both at Lick and at AAT are in good agreement (as was already implied by Fig. 3). For such clusters we adopt a simple mean of the two estimates. Finally, in Figure 8 we present a plot of $\bar{\Delta}$ as a function of adopted metallicity for our 20 fundamental calibrating clusters. Examination of the figure shows that the dependence is nonlinear and that our index is less robust in the metal-weak than in the metal-rich regime: a typical measurement error of ± 0.010 in Δ translates to ± 0.2 dex near [Fe/H] $= -2.0$ but to ± 0.02 dex near [Fe/H] $= -1.0$. Of (course the true systematic uncertainties may be larger than these purely formal errors.) The relationship sketched in the diagram is our freehand fit to the points, and on the basis of that relationship we have determined metallicities for all the clusters studied; the final values are given in Table 6.

g) Galaxies

In addition to observing 24 globular clusters at Lick, we also acquired spectra for the nuclei of six galaxies. In Table 7 we present the measured indices, derived as for the clusters. Figure 9 suggests that the galaxies are more metal-rich in general than the globular clusters. However, for metallicities greater than

TABLE 6

CLUSTER METALLICITIES

NGC	[Fe/H]	NGC	[Fe/H]
1851.....	-1.09 ± 0.01	6362.....	-0.92 ± 0.04
1904.....	-1.70 ± 0.23	6402.....	-1.15 ± 0.03
2298.....	-1.67 ± 0.24	6541.....	-1.42 ± 0.04
5024.....	-2.04 ± 0.26	6626.....	-1.07 ± 0.01
5272.....	-1.45 ± 0.01	6712.....	-1.00 ± 0.03
5634.....	-1.46 ± 0.05	6723.....	-1.09 ± 0.01
5904.....	-1.28 ± 0.01	6752.....	-1.35 ± 0.04
5927[a].....	$[-0.65 \pm 0.04]$	6779.....	-1.41 ± 0.03
5946.....	-1.26 ± 0.05	6809.....	< -2.0
5986.....	-1.34 ± 0.02	6838.....	-0.83 ± 0.05
6093.....	-1.57 ± 0.03	6864.....	-1.11 ± 0.03
6171.....	-0.90 ± 0.05	6934.....	-1.27 ± 0.01
6205.....	-1.33 ± 0.01	6981.....	-1.26 ± 0.02
6218.....	-1.21 ± 0.02	7006.....	-1.32 ± 0.02
6229.....	-1.19 ± 0.01	7078.....	-2.11 ± 0.09
6254.....	-1.46 ± 0.02	7089.....	-1.41 ± 0.07
6273.....	-1.35 ± 0.02		
6341.....	-1.93 ± 0.13		
6352.....	-0.85 ± 0.04		
6356[a].....	$[-0.75 \pm 0.02]$		

[a] More metal-rich than our most metal-rich calibrator, NGC 6838.

TABLE 7

INDICES FOR GALAXIES OBSERVED AT LICK

NGC	Messier	Δ	H10	H9	Hζ	CN	HK	Hδ	Ca	G	Hγ	Hβ	Mg	MH	FC	Weight
221.....	32	0.561	0.069	0.167	0.061	0.134	0.280	−0.003	0.007	0.101	0.013	0.064	0.050	0.061	0.041	3.9
224.....	31	0.700	0.185	0.173	0.090	0.177	0.250	−0.040	0.008	0.068	−0.014	0.046	0.101	0.072	0.058	2.6
4472.....	49	0.653	0.182	0.171	−0.041	0.145	0.223	−0.007	0.027	0.115	−0.035	0.045	0.104	0.084	0.032	2.0
4486.....	87	0.611	0.142	0.176	−0.012	0.208	0.264	−0.041	0.031	0.132	−0.041	0.030	0.097	0.094	0.059	1.9
4594.....	104	0.648	0.009	0.354	−0.025	0.304	0.275	0.004	0.042	0.117	−0.031	0.045	0.105	0.080	0.048	1.9
5194.....	51	0.344	0.068	0.134	0.127	0.064	0.186	0.029	0.000	0.103	0.051	0.041	0.072	0.050	0.045	1.8

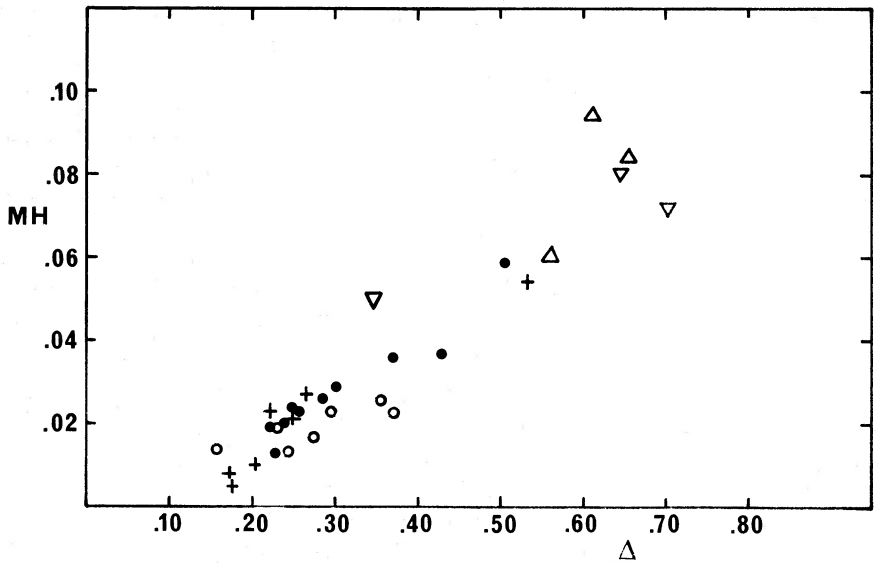

FIG. 9.—Correlation between MH and Δ for globular clusters and galaxies observed at Lick. Symbols for clusters represent relative weights in the sense described in the legend for Fig. 6. Open triangles represent spiral (▽) and elliptical (△) galaxies.

[Fe/H] = −0.5 we lack fundamental calibrators with which to define the abundance relations. We therefore calibrate the galaxy metallicities by relating our MH index to Burstein's (1979) treatment of the $(Mg)_0$ index originally defined by Faber (1973). As a first step, we improve our estimates of the MH index by reducing our measurements of the Δ parameter and the G index to MH, as shown in Figure 10. From that figure we predict, from Δ and G, equivalent values of MH, finally averaging these (with half-weight) with the direct measurements of MH itself to yield $\overline{MH}$. We next recognize the close similarity in definition of our MH index and Burstein's $(Mg)_0$ index: the wavelength windows defining the feature are comparable (our baseline being rather shorter), although Burstein's index is expressed in magnitudes. The good agreement between the indices is shown in Figure 11, where we plot Burstein's values against our weighted $\overline{MH}$ estimates for four globular clusters and three galaxies in common. Using the derived relationship given in the figure, we convert our $\overline{MH}$ index to $(Mg)_0$ equivalents for all the metal-rich objects studied.

For a final calibration, we rely, as did Burstein, upon Mould's (1978) theoretical investigation of the dependence of magnesium feature strength upon metal abundance. Burstein

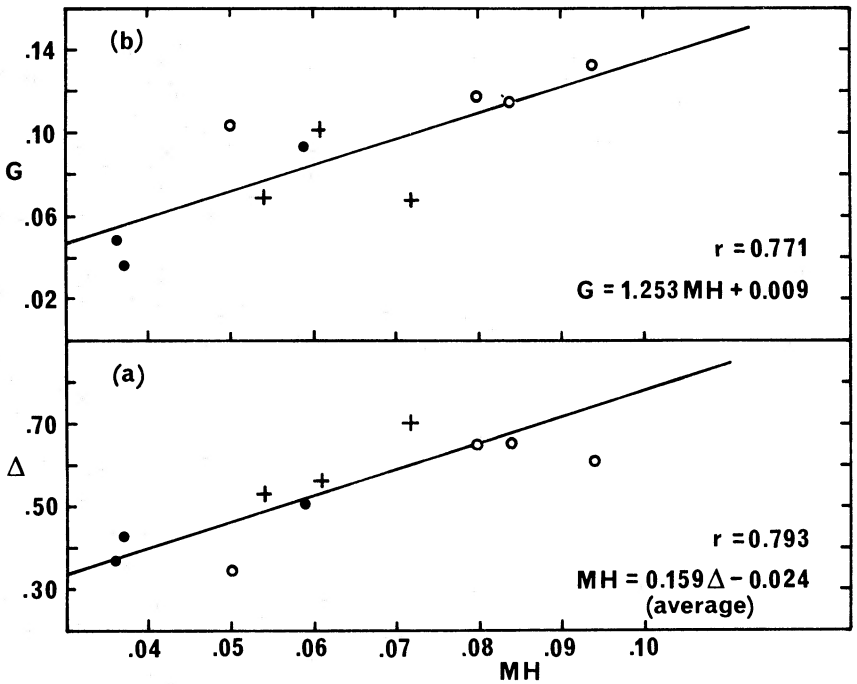

FIG. 10.—Correlation (*a*) between Δ and MH and (*b*) between G and MH for four metal-rich globular clusters and six galaxies observed at Lick. As in Fig. 6, plus signs represent the highest weight data, filled circles the lowest. The weighted regression line in panel *a* is an average of the two senses; that in panel *b* assumes all the error to be in G.

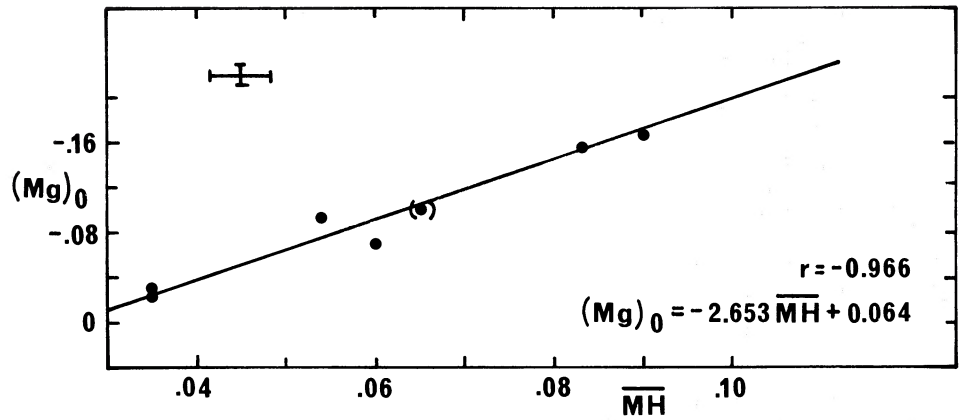

FIG. 11.—Relationship between $(Mg)_0$ as tabulated by Burstein (1979) and our $\overline{MH}$ index for globulars and galaxies in common. A typical error bar is shown at the upper left, the error bar in $\overline{MH}$ being that implied by the various determinations of MH described in § IV*g*. The point in parentheses is less precise, according to Burstein. For the regression the data were assigned the extrinsic weights given in Tables 3A and 7.

in fact slightly shifted the zero point of Mould's theoretical calibration, still within Mould's quoted error, the better to fit his observations of metal-rich globular clusters. Of course the recent revisions in the globular cluster abundance scale are felt directly here, and we must reconsider the quality of the zero-point agreement. Mould quoted an estimated uncertainty of ± 0.2 dex in the zero point of the calibration; we show in Figure 12 that a shift of about 0.3 dex in [Fe/H] brings the relationship into good agreement with the most metal-rich clusters on the new scale. We adopt the relationship plotted in the figure. The metallicities which we derive for the galaxy nuclei are summarized in Table 8. It must be noted that our observations of NGC 4594 and NGC 5194 may be subject to contamination from the Population I component of these spiral galaxies despite our efforts to center the entrance apertures on the nuclear parts.

V. DISCUSSION AND COMPARISON WITH OTHER RESULTS

Having derived abundances for 36 galactic globular clusters, we now compare our results with recent work by other authors. We begin by assessing our sensitivity to the known variation in horizontal-branch strength from cluster to cluster,

TABLE 8

METALLICITIES OF GALAXIES

NGC	Messier	[Fe/H]
221	32	-0.13 ± 0.04
224	31	-0.06 ± 0.15
4472	49	$+0.13 \pm 0.02$
4486	87	$+0.24 \pm 0.11$
4594	104	$+0.11 \pm 0.03$
5194	51	-0.32 ± 0.16

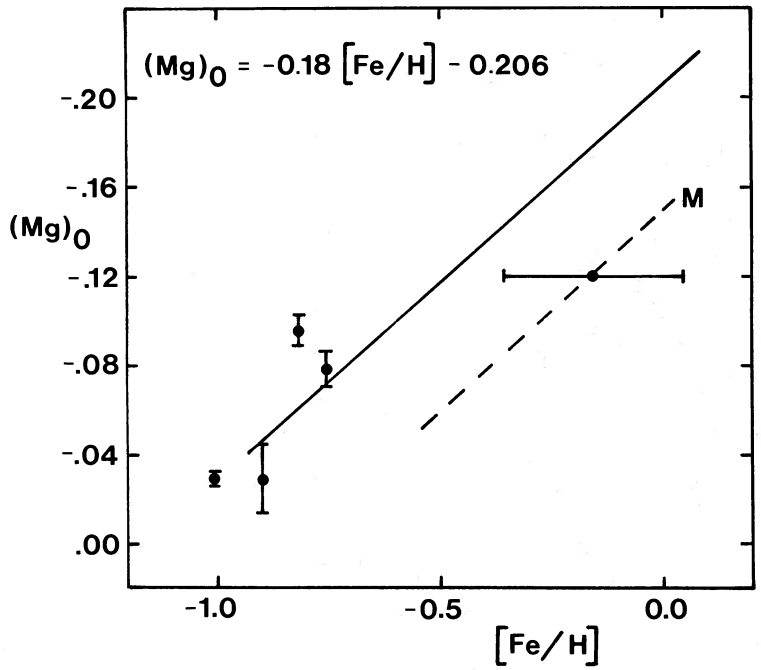

FIG. 12.—Calibration of $(Mg)_0$ as a function of metallicity. Data for four metal-rich clusters are plotted. The dashed line represents Mould's (1978) theoretical relationship (labeled *M*) with its associated uncertainty (superposed error bar). Our adopted calibration, the equation of which is given, is shown as a solid line; it has been displaced to give a better match to the data points for the metal-richest clusters.

for this variation has been identified as the source of a systematic error in the metallicities derived by Zinn (1980), as we shall describe in § V*b*.

a) Our Insensitivity to Horizontal-Branch Morphology

Our Δ parameter measures the size of the continuum break near 4000 Å and may be sensitive to dilution by excess ultraviolet light from hot stars. If the effect is important, we expect the Δ index to be too small and thus to imply systematically lower metallicities for clusters with anomalously strong blue horizontal branches (BHB) for their metallicity. The Δ index is easily measured with high precision, and abundance estimates based upon it should formally enter the averaging with high weight. However, partly to preclude such systematic effects (but also because of the extra sensitivity of the asymmetric Δ feature to errors in the reddening and extinction corrections) we gave it a weight merely equal to that of the mean of other metallicity determinations, as noted in § IV*d*. None the less, our results must be tested for any important residual bias.

To this end, we have evaluated Δ both including and excluding the direct measurement of Δ itself. Figure 13 shows that these estimates are in excellent agreement in general; more important, it also shows that there is no dependence upon horizontal-branch morphology, even in the intermediate metallicity regime, where the second-parameter effect is most pronounced. Moreover, application of our calibrating relationship to the different estimates of $\bar{\Delta}$ reproduces the input values of [Fe/H] for the calibrating clusters to good accuracy irrespective of horizontal-branch morphology.

Does the general insensitivity of our methods to horizontal-branch morphology preclude the identification of anomalous horizontal-branch clusters? To test this possibility, we compared the abundances inferred from hydrogen line strengths alone with those derived from all nonhydrogenic species. In the AAT data, which have formally determined error estimates, we have identified four clusters for which $[Fe/H]_H$ and $[Fe/H]_{non\text{-}H}$ differ by more than 3 times the combined errors. Table 9 summarizes these results, quoting as well the horizontal-branch morphology. Inspection of the table reveals that there is no consistent sense: two clusters with very blue horizontal branches (NGC 6541, NGC 6752) exhibit opposite behavior at comparable levels of significance. Apparently the formal disagreements reflect the slightly optimistic nature of the quoted errors in individual metallicity determinations rather than any astrophysically significant difference. Certainly we detect no anomalous examples such as have been reported on the basis of Hβ line strengths in some of the globular clusters in M31 (Burstein *et al.* 1981).

TABLE 9

CLUSTERS WITH ANOMALOUS HYDROGEN LINE INDICES

Cluster	Sense of Difference	Significance	HB[a]
NGC 6352.....	H lines weak	3.2 σ	0.78
NGC 6541.....	H lines weak	4.1 σ	0.13
NGC 6752.....	H lines strong	3.2 σ	0.10
NGC 6723.....	H lines weak	3.7 σ	0.54

[a] Alcaino 1979. HB is the ratio of the number of stars lying on the horizontal branch to the red of the RR Lyrae gap to the total of all stars lying on the horizontal branch to either the red or the blue of the gap; thus HB = $R/(B + R)$.

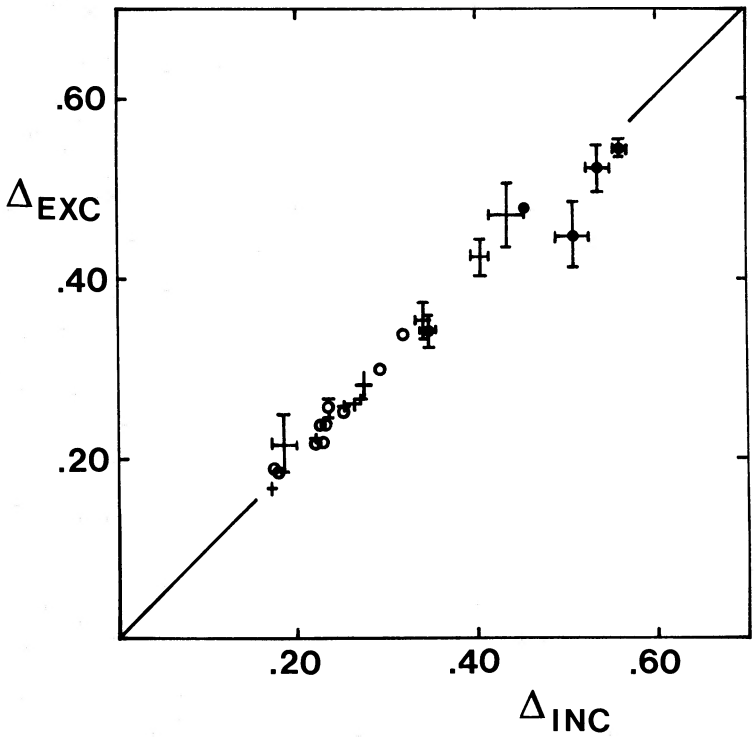

FIG. 13.—Comparison between our estimates of $\bar{\Delta}$ evaluated both including (*abscissa*) and excluding (*ordinate*) the direct measurement of Δ itself. Open symbols represent clusters with extremely blue horizontal branches (HB < 0.20; Alcaino 1979); filled symbols represent clusters with extremely red horizontal branches (HB > 0.70). The diagonal line represents the identity relationship.

b) Comparison with Zinn (1980)

Zinn's adopted scale predates the important recent changes summarized by Pilachowski (1984) for the well-studied metal-rich clusters. In the present study, we have adopted those revisions, and of course there can be no exact agreement between Zinn's scale and our own. However, a detailed comparison is important: Zinn's observations represent a large body of data on a homogeneous system, and we must test for potential problems within it. Indeed, a problem has been identified: various authors (Brodie and Hanes 1981; Frogel, Cohen, and Persson 1983; Pilachowski 1984) have pointed out that globular clusters of intermediate metallicity which have strong blue horizontal branches are measured by Zinn to be more metal-poor than they are by other authors, once scale differences are compensated for.

The plausible explanation is the sensitivity of Zinn's Q_{39} index to excess ultraviolet light shortward of the discontinuity. Pilachowski (1984) has put Zinn's metallicities onto her new scale, explicitly correcting individual values for the contaminating effects of the horizontal branch where necessary. In Figure 14 we show the good agreement between our results and those of Zinn as modified by Pilachowski. Clusters with extremely blue horizontal branches are indicated; they do not disagree with the general run of points. We have seen that our metallicities are insensitive to BHB morphology; thus Figure 14 implies that Pilachowski's modifications to Zinn's determinations make them now correctly insensitive to BHB morphology. We confirm the important lesson that Zinn's raw measurements must be adjusted for the spectral dilution of the Q_{39} index by excess ultraviolet light before they may be employed as indicators of cluster metallicity.[1]

c) Comparison with Frogel, Cohen, and Persson (1983)

In Figure 15 we compare the metallicities tabulated by Frogel, Cohen, and Persson (1983) with those derived in the present study. Good agreement is seen for clusters more metal-poor than [Fe/H] = −0.8. The infrared observations which constitute the work of Frogel *et al.* should be immune to the horizontal-branch problems described in § V*b*, as those authors indeed emphasize in independently pointing out the effect in Zinn's results. Figure 15 thus reconfirms our insensitivity to the effect.

There is, however, a pronounced separation of the scales at the metal-rich end. This reflects the fact that Frogel, Cohen, and Persson (1983) adopted as calibrating clusters two which were taken to be very metal-rich: NGC 5927, at [Fe/H] = −0.1, and NGC 6352, at [Fe/H] = −0.3. Our most metal-rich calibrating cluster, NGC 6838, lies at [Fe/H] = −0.8 according to Pilachowski (1984), a value with which Frogel *et al.* agree (they adopt −0.75). The three most discrep-

[1] It may be worthwhile to repeat a remark made in a early version of this paper (AAO Preprint 198) in which we calibrated cluster metallicities in terms of the "old" scale. Since that scale was almost identical with Zinn's, a straightforward intercomparison was possible. We found a striking nonlinearity in the region of intermediate metallicities, and traced this to the fact that of Zinn's five calibrators at that abundance, no fewer than four were of extremely red horizontal-branch morphology. This piece of bad fortune exacerbated the

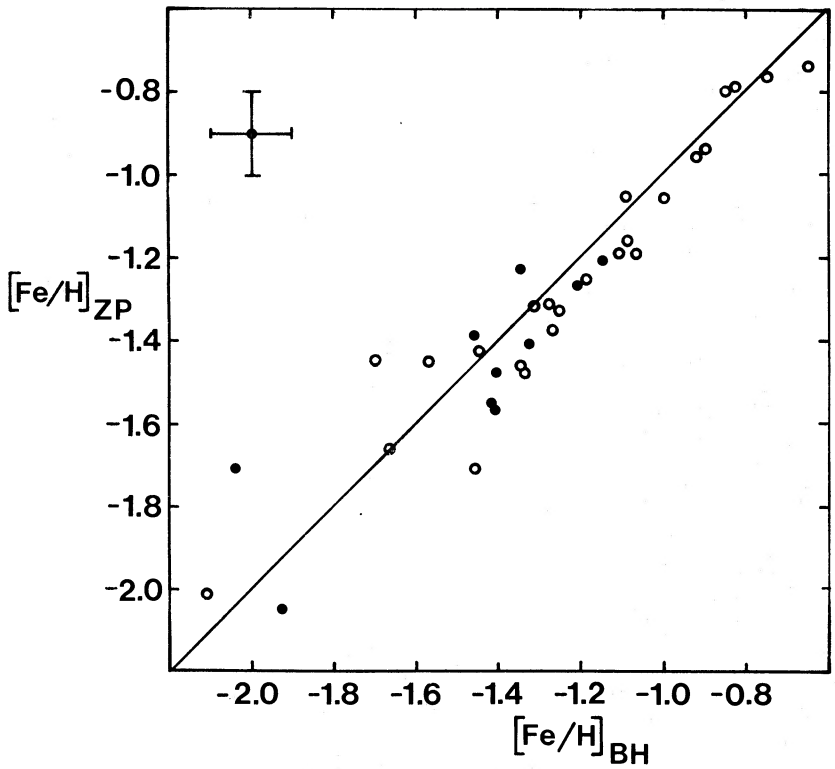

FIG. 14.—Comparison between our estimates of cluster metallicity and those derived from Zinn's (1980) Q_{39} index, as put on the new cluster metallicity scale by Pilachowski (1984) and as corrected by her for the effects of the dilution of the index by excess ultraviolet flux in clusters with anomalously strong blue horizontal branches (the filled symbols represent such BHB clusters). The diagonal line represents the identity relationship. The scales are in good agreement, although there is a small (~0.05 dex) zero-point difference.

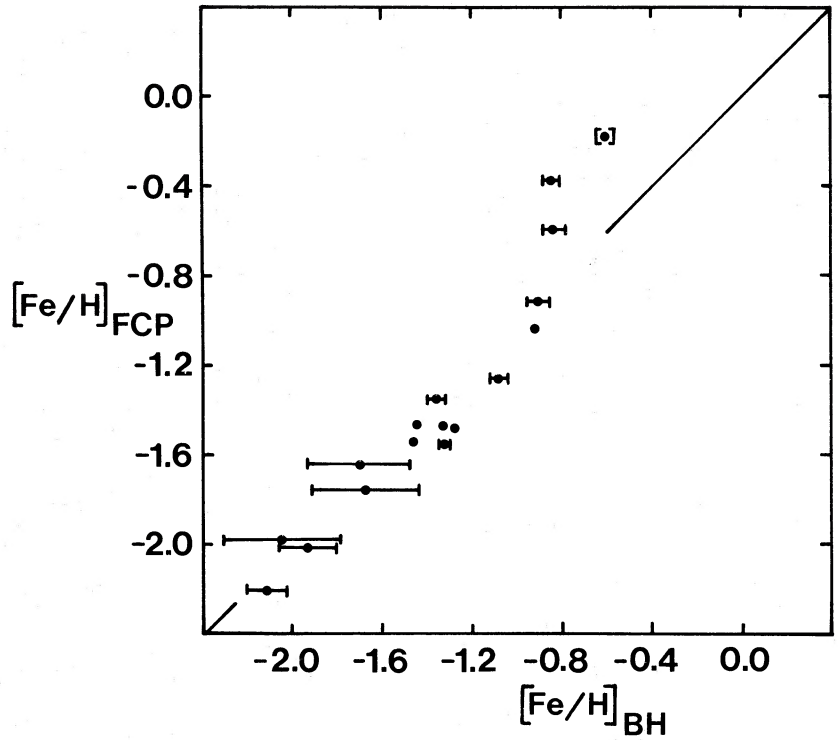

FIG. 15.—Comparison of the metallicities derived by us and by Frogel, Cohen, and Persson (1983) for clusters common to the two studies. The line is the identity relationship. The error bars in our determinations are the formal ones implied by the internal agreement among various indices, as described in the text. The true systematic uncertainties must be larger.

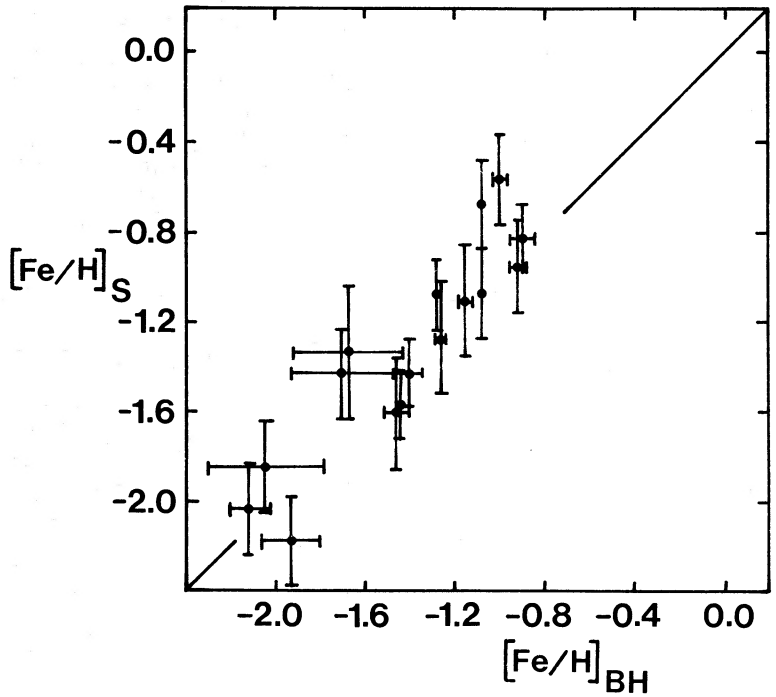

FIG. 16.—Comparison of the metallicities derived by us with those tabulated by Smith (1984) for clusters common to the two studies. The line is the identity relationship.

ant points in Figure 15, corresponding to NGC 5927, NGC 6352, and NGC 6838, exit the calibration of Frogel *et al.* with final values of [Fe/H] = −0.18, −0.38, and −0.60, respectively. However, our measurements of $\bar{\Delta}$ (Table 5) indicate that NGC 6352 is comparable to or in fact slightly more metal-poor than NGC 6838. (Note that we find NGC 5927 to be stronger-lined than our most metal-rich calibrator; thus our abundance estimate for it depends upon the arguments of § IV*g*.) We do not believe that our spectra for the half-dozen most metal-rich clusters common to both studies support the wide range in metallicities given by Frogel, Cohen, and Persson (1983) for those six. In this we agree with Pilachowski (1984), who quotes [Fe/H] = −0.74 and [Fe/H] = −0.8 for NGC 5927 and NGC 6352, respectively; note, however, that we did not use those two as calibrating clusters, since they do not appear under the heading "Calibration" in Pilachowski's Table 1.

d) Comparison with Smith (1984)

In Figure 16 we plot our metallicities against those derived by Smith (1984), whose estimates are based upon measurements of the ΔS parameter for RR Lyrae stars in clusters. Good agreement is seen, although there are no very metal-rich clusters common to the two studies.

VI. SUMMARY AND CONCLUSIONS

We have derived absolute abundances for 36 Galactic globular clusters through analysis of the strengths of several prominent absorption features in low-dispersion spectra of their integrated light. The metallicities which we derive are insensitive to horizontal-branch morphology. Our scale is consistent with the suggestion (Brodie and Hanes 1981; Frogel, Cohen, and Persson 1983; Pilachowski 1984) that Zinn's (1980) scale suffers from a systematic error which originates in the sensitivity of his Q_{39} index to cluster horizontal-branch morphology. Our results are in good agreement with those in several recent studies, with the exception that we do not find the most metal-rich clusters to be as metal-rich as is indicated by Frogel, Cohen, and Persson (1983); in this we agree with Pilachowski (1984).

On the basis of a theoretical calibration of the high-metallicity regime we have derived abundances for six galaxies. The extension of our methods beyond the metallicity range of Galactic globular clusters will be applied in a subsequent paper (Hanes and Brodie 1986) to a study of the globular clusters associated with the giant elliptical galaxy M87. In the future, a more general application of our technique or similar ones to the spectra of extragalactic globular cluster systems observed with the Hubble Space Telescope will permit the study of the dynamical and chemical history of the oldest stellar components of galaxies.

We are pleased to acknowledge generous grants of observing time from the committees responsible for the Lick Observatory and the Anglo-Australian Telescope. Donald Osterbrock encouraged us originally to think of observing at Lick, Sandy Faber gave us helpful advice, and Rem Stone made the whole effort a success with technical assistance and encouragement. At the AAT we were supported in the usual excellent fashion. We especially thank Frank Freeman for his meticulous and enthusiastic attention to the exigencies of the observing program. We are grateful for the constructive and thoughtful comments of an anonymous referee, whose detailed criticisms led us to rework our data in light of the recent changes in the globular cluster metallicity scales; the paper has benefited greatly as a result. The work described in this paper was supported in part by a Natural Science and Engineering Research Council of Canada operating grant awarded to D. A. H.

REFERENCES

Alcaino, G. 1979, *Vistas Astr.*, **23**, 1.
Bahcall, J. 1984, in *IAU Symposium 113, The Dynamics of Star Clusters*, ed. P. Hut (Dordrecht: Reidel), in press.
Bessell, M. S. 1983, *Pub. A.S.P.*, **95**, 94.
Brodie, J. P. 1980, Ph D. thesis, Cambridge University.
Brodie, J. P., and Hanes, D. A. 1981, in *IAU Colloquium 68, Astrophysical Parameters for Globular Clusters*, ed. A. G. Davis Philip and D. S. Hayes (Schenectady: Davis), p. 381.
Burstein, D. 1979, *Ap. J.*, **232**, 74.
Burstein, D., Faber, S. M., Gaskell, C. M., and Krumm, N. 1981, in *IAU Colloquium 68, Astrophysical Parameters for Globular Clusters*, ed. A. G. Davis Philip and D. S. Hayes (Schenectady: Davis), p. 441.
Cohen, J. G. 1980, *Ap. J.*, **241**, 981.
———. 1983, *Ap. J.*, **270**, 654.
de Vaucouleurs, G., de Vaucouleurs, A., and Corwin, H. G. 1976, *Second Reference Catalogue of Bright Galaxies* (Austin: University of Texas Press).
Faber, S. M. 1973, *Ap. J.*, **179**, 731.
Freeman, K. C., and Norris, J. 1981, *Ann. Rev. Astr. Ap.*, **19**, 319.
Frogel, J. A., Cohen, J. G., and Persson, S. E. 1983, *Ap. J.*, **275**, 773.
Hanes, D. A., and Brodie, J. P. 1986, *Ap. J.*, **300**, 279.
Harris, W. E. 1983, *Pub. A.S.P.*, **95**, 569.
Harris, W. E., and Racine, R. 1979, *Ann. Rev. Astr. Ap.*, **17**, 241.
Hesser, J. E., Harris, H. C., van den Bergh, S., and Harris, G. L. H. 1984, *Ap. J.*, **276**, 491.
Johnson, H. L. 1968, in *Stars and Stellar Systems*, Vol. **7**, *Nebulae and Interstellar Matter*, ed. B. M. Middlehurst and L. H. Aller (Chicago: University of Chicago Press), p. 167.
Madore, B. F. 1980, in *Globular Clusters*, ed. D. A. Hanes and B. F. Madore (Cambridge: Cambridge University Press), p. 21.
Mould, J. R. 1978, *Ap. J.*, **220**, 434.
Norris, J. 1980, in *Globular Clusters*, ed. D. A. Hanes and B. F. Madore (Cambridge: Cambridge University Press), p. 113.
Oke, J. B. 1974, *Ap. J. Suppl.*, **27**, 21.
Peterson, R. C. 1983, *Pub. A.S.P.*, **95**, 98.
Pilachowski, C. A. 1984, *Ap. J.*, **281**, 614.
Sandage, A. R. 1973, *Ap. J.*, **183**, 711.
Smith, H. A. 1984, *Ap. J.*, **281**, 148.
van den Bergh, S., and Henry, R. C. 1962, *Pub. David Dunlap Obs.*, **2**, 281.
Zinn, R. 1980, *Ap. J. Suppl.*, **42**, 19.

JEAN P. BRODIE: Space Science Laboratories, University of California, Berkeley, CA 94720

DAVID A. HANES: Astronomy Group, Physics Department, Queen's University at Kingston, Kingston, Ontario K7L 3N6, Canada